Physics approaches to natural locomotion: Every robot is an experiment

6

Yasemin Ozkan Aydin, Jennifer M. Rieser*, Christian M. Hubicki*, William Savoie*, Daniel I. Goldman**
*School of Physics, Georgia Institute of Technology, Atlanta, GA, United States

6.1 Introduction

In 1990, Eric Krotkov authored a paper "Active perception for legged locomotion: every step is an experiment" [1], where he discussed how legged robots could improve performance on natural terrain by "stepping on and kicking things" as a perception task. When integrated with vision, this approach could lead to better robot locomotion. In addition, such processes could also improve understanding of the terrain.

Krotkov's vision does not shy away from novel environmental interactions; unfortunately, such an approach has not been the paradigm in robotics and control. Speaking broadly, these disciplines tend to treat the robot and environment as highly controlled, sterile systems with simple interaction models. However, this approach is running up against limits; as seen in Fig. 6.1, robots do and will face terrestrial environments that are not controlled, not deterministic and whose physics (needed for modeling interactions) is unknown.

How should we proceed with the task of discovering principles for robust movement in complex environments, particularly when movement entails organizing huge numbers of degrees of freedom? One approach, largely stemming from the dynamical systems community, and applied to living systems, is to seek low-dimensional limit cycle dynamics or representations, called templates in the language of [2]. When a locomotor's many degrees of freedom are controlled to target a template dynamics, the systems can accrue benefits in speed, stability, and energy use. This paradigm has proved useful to unite biological locomotion principles (e.g., inverted pendulum, bouncing inverted pendulum, inertial righting). Once templates are discovered, the next job is to "anchor" these in physiologically realistic models.

While the template approach has been useful in generating biological control hypotheses, it has received less application in terrestrial robots—notable exceptions are bouncing and walking robots that use dynamical stability properties of hopping and sustained falling to simplify control [3, 4, 4a, 4b]. We posit that this is largely due to the previously mentioned legacy of robotics and the engineering focus—robots are treated as afterthoughts once the control scheme has been developed mathematically and the environment has been controlled. Further robot design and fabrication

Robotic Systems and Autonomous Platforms. https://doi.org/10.1016/B978-0-08-102260-3.00006-8

Fig. 6.1 Autonomous robots exhibit increased mobility on a variety of complex terrains. (A) Hexapod robot "RHex" moving over rough terrain; (B) Atlas, designed to operate outdoors and inside buildings; (C) "Kilobots" are programmed to exhibit complex swarming behaviors; (D) modular snake robot that was used in Mexico City earthquake to search for survivors. (A) credit: Kod*lab, University of Pennsylvania. (B) credit: Boston Dynamics. (C) credit: Self-Organizing Systems Research Group, Harvard University (D) credit: Biorobotics Laboratory, Carnegie Mellon University Robotics Institute.

has been expensive and time-consuming, decreasing design iteration times, and creative parameter space exploration.

Here then is our plea and challenge: treat the robots as experiments and conduct physics on them. The physics approach is simply to learn about a complex system by performing high-quality experiments, constructing simplified models, and subjecting these models to tests outside the expected parameter range. For lack of a better name, we refer to this process as experimental robotics or "robophysics" [5]. For example, when applied to locomotion, the performance of novel legged robot platforms on granular media no longer becomes the sole focus of the discipline; discovery of new fundamental principles of movement—for example, the importance of substrate solidification [6] or fluidization [7]—is only revealed by systematic tests.

The ability to treat robots as experimental tools has been made easier due to the development of additive manufacturing techniques (e.g., 3D printing), effective

and low-cost actuators and sensors, and improved power management; we are now able to design, build, and, if needed, rapidly redesign low-cost robots. Although these robots are not durable and suitable for a long-lasting interaction, they can be run in systematic and automated experiments to rapidly explore a wide range of parameter space and determine the capabilities of the robots' locomotive configuration.

In this chapter, we will discuss four examples in which using robots as experimental tools is bearing fruit. We will begin with an example in which a simple legged robot interacts with granular media and produces surprising complexity such that the environment becomes time dependent. Here, our previously developed tools (e.g., resistive force theory (RFT) [8]) are not yet applicable, and computer simulation is too time consuming, so we use robots to probe the dynamics and develop novel control schemes. We will then discuss how we are beginning to use robots to discover principles of interaction in heterogeneous environments, regimes where they tend to fail. We will focus on a snake-like robot and show that when moving through regular arrays of obstacles, it produces patterns reminiscent of wave-like diffraction. This can be useful for future anticipatory control schemes. Next, we will show how simple changes in actuation of a robot can lead to effective mechanical interaction with heterogeneous environments, enabling transit in situations which would otherwise require sophisticated controls. We will close with a discussion of recent efforts to create robots and robotic materials created from functional robotic components, in effect modeling an important aspect of living systems.

6.2 Terrestrial locomotion on flowable substrates

Movement through even seemingly simple terrestrial environments such as homogeneous sand can be challenging. With each footstep, the material can deform and flow, influencing the stability of the locomotor as well as the ability to generate propulsive forces necessary to sustain movement. Previous work adapted RFT, originally developed to predict the speed of swimmers in highly dissipative viscous environments [9], to apply to movement within granular materials (another highly dissipative medium). RFT was able to successfully predict the speed of a lizard swimming within granular material [10]. Subsequent studies have shown that RFT is able to predict performance of locomotors of arbitrary geometry moving through granular media [6, 11, 12]. Recent work by Askari and Kamrin provides a theoretical understanding of RFT and predicts its applicability to a wide range of highly dissipative environments [13].

To generate movement, locomotors often perform cyclic patterns of self-deformation, which, when coupled to an external environment, can produce movement. Shapere and Wilczek [16] developed a framework that relates body-frame deformations to displacements in the world-frame for highly dissipative environments. This geometric approach was extended to understand the principles of effective locomotion within granular media in which inertial forces were small relative to frictional forces and applied to design gaits for many systems [14, 17–20]. It was also shown that, despite the lack of fundamental equations of motion, this approach can also empirically generate locomotion patterns for high-dimensional systems in a

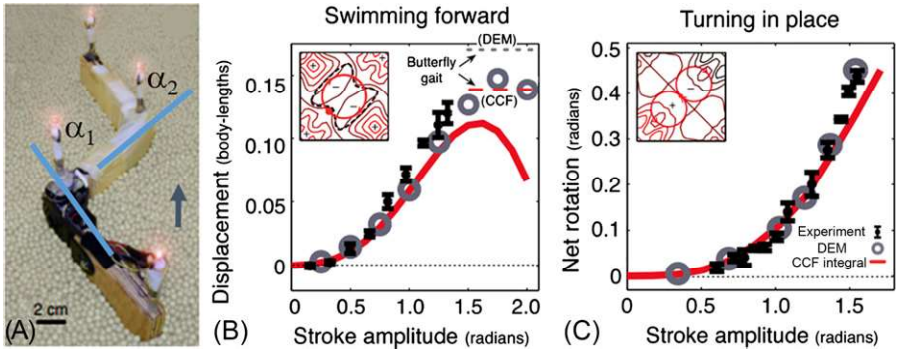

Fig. 6.2 Comparison of geometric mechanics and robophysical sand-swimming. (A) A three-link robot at rest on a bed filled with 6 mm diameter plastic spheres. (B) Displacement per cycle as a function of stroke amplitude. The *red curve* shows the displacement predicted by constraint curvature function (CCF) surface integrals for circular gaits of varying stroke amplitude (in radians, the maximum angle swept out by each arm of the robot). The *inset* shows the CCF and an example circle gait (*red*) as well as the "butterfly gait" (*dashed black*), which shows the gait that produces the maximum displacement. In the main plot, DEM and CCF-predicted displacements are indicated by *dashed horizontal lines* on the right side of the plot. *Black points* with errorbars indicate experimental circle-gait displacements, and *gray circles* show corresponding DEM predictions. (C) Net rotations predicted from CCF (*red*), DEM (*gray*), and experimental measurements (*black*) for figure-8 gaits of different stroke amplitudes (an example of a figure-8 gait is outlined as the *red curve* in the *inset*) [14].

granular medium (Fig. 6.2). However, it is not yet clear if this approach can be used in situations in which the environment is time dependent, that is, has hysteretic effects. On granular substrates in particular, repeated contact with the ground creates persistent surface disturbances, which can influence subsequent steps. This terrain hysteresis is particularly problematic as locomotion success is quite sensitive to substrate properties [12, 21]. It has been hypothesized that animals such as turtles and mudskippers have evolved morphological adaptations (e.g., flexible flippers) to accommodate granular materials [19, 21–23]. Further, collaborative work on tetrapod locomotion using geometric mechanics and computer models suggests that coordinated body bending can improve performance on challenging substrates [20, 24].

Here, we take a robophysical approach to exploring morphologies and gait patterns for tetrapod locomotion on flowable terrain. Specifically, we systematically study how a back-bending degree of freedom can assist ambulation on a sloped granular surface [5]. To serve as a robophysical tetrapod model, we built an open-loop servo-driven 3D-printed robot that has four limbs, an actuated trunk, and an active tail (Fig. 6.3A). Each limb has a proximal motor that actuates the leg vertical position and a more distal motor that controls the step size. A central joint in the body controls horizontal body bending (Fig. 6.3A and B).

At the beginning of each experiment, the robot is placed on a trackway filled with poppy seeds; see Fig. 6.3C–G. After this the robot executes a predefined gait pattern. For this study, we command a symmetric diagonal gait, where each forelimb makes

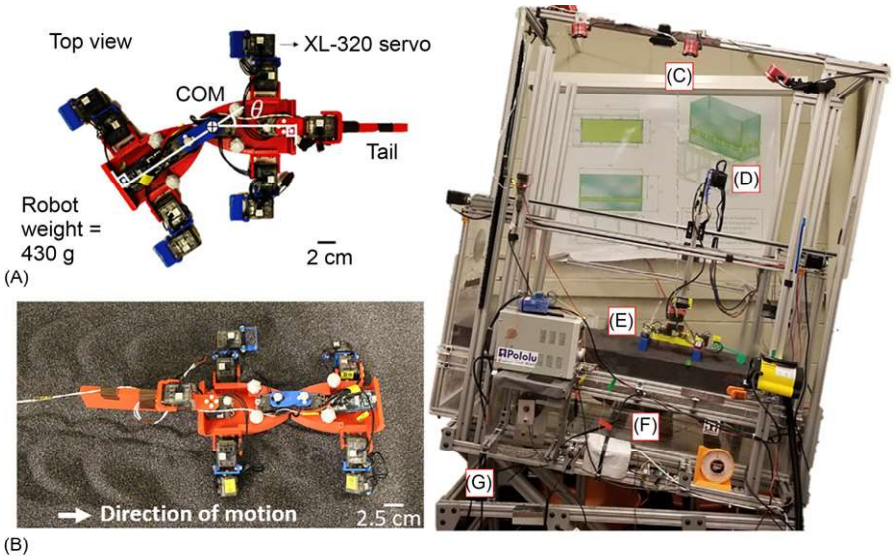

Fig. 6.3 Study of tetrapod locomotion on granular media. *Right panel*: The Systematic Creation of Arbitrary Terrain and Testing of Exploratory Robots (SCATTER) [15] system allows for automated three-axis manipulation of a robot traversing a granular substrate with specified surface incline. (A) Top view of the salamander robot. Each leg has two Dynamixel XL-320 servos. A servo motor in the center of the back connects two body segments and enables actuation of the body angle θ that ranges from 0 degree (straight back) to 90 degrees (maximally bent back). (B) The salamander robot moves in poppy seeds. Indentations in the poppy seeds (here, to the left of the robot) are footsteps that were created by the robot throughout the execution of a few gait cycles (here, the robot walked from left to right). (C) Optitrack vision capture system. (D) Openbuilds three-axis gantry system. (E) Electromagnetic gripper. (F) Fluidized bed trackway filled with poppy seeds. (G) Firgelli tilting actuator.

contact with the terrain simultaneously with its counterpart contralateral hindlimb (e.g., left forelimb synchronized with right hindlimb). Limb and body positions are recorded as the robot traverses the trackway via motion capture. When the robot reaches the end of the trackway, a three-axis gripper locates the robot and returns it to the initial position. While the robot is being returned to the initial position, the granular material is fluidized to erase the tracks and reset the surface to a loosely packed state.

We systematically varied the amplitude of the body angle, θ, from 0 degree to 90 degrees and measured the performance of the robot (the step length, ΔX). These repeated experiments revealed that step length increased with larger body bending motions; however, for $\theta = 75$ degrees, ΔX decreased because the hind legs interacted with ground disturbed by previous steps (see Fig. 6.4A and B). For comparison, we tested locomotion performance on both hard ground and our poppy seed granular preparation. On hard ground at 0- and 10-degree slopes, the feet did not slip and

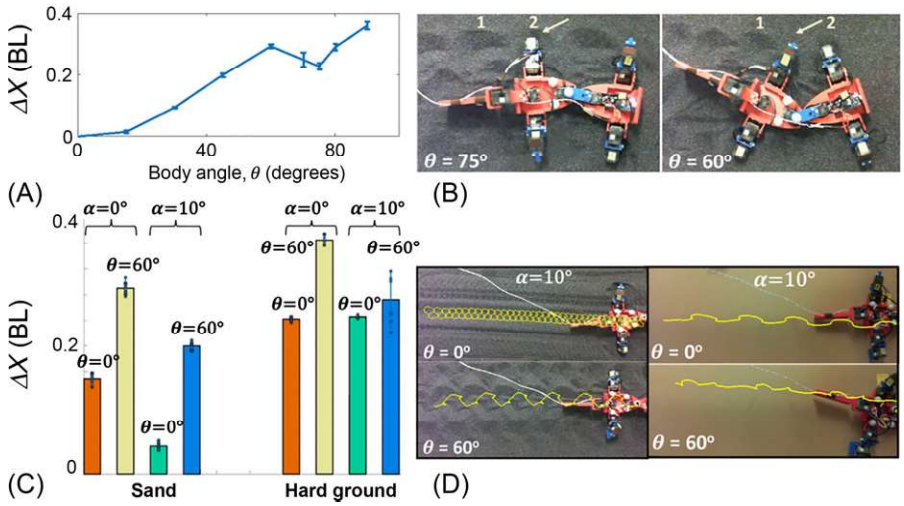

Fig. 6.4 Performance of a tetrapod robot with an actuated body joint moving on granular media. (A) Amplitude of body bending θ (changing from 0 degree to 90 degrees) versus step length (cm). (B) Tracks of the robot in poppy seeds for $\theta = 75$ degrees (*left*) and $\theta = 60$ degrees (*right*); the numbers show the ground interaction point of the hind left foot for two successive foot placements. (C) Step length, ΔX, of the robot while moving on granular media and hard ground. The slope of the bed is changed from 0 degree to 10 degrees and the body angle amplitude is changed from 0 degree to 60 degrees. (D) Corresponding trajectories of the robot while moving on $\alpha = 10$ degrees inclined granular (*left*) and hard surface (*right*). The *yellow lines* represent the trajectory of the CoM during the run.

the added body bending increased the effective step length by ~50% (on level ground) and ~1% (on 10-degree slopes). On granular material, the robot's step length decreased by ~40% (on level ground) and ~80% (on 10-degree slopes) relative performance on hard ground. Back bending restored performance on granular material, leading to step lengths only ~20% (on level ground) and ~25% (on 10-degree slopes) less than those on hard ground (Fig. 6.4C and D). The results highlight that robot performance on granular media can be greatly improved by the proper coordination of body bending with limb placement. We suspect that this improvement is due to avoidance of previously disturbed material and enhancing propulsive forces.

These results provide insight into how hysteretic effects of soft substrate influence ambulatory locomotion. In contrast to our previous work, which highlighted how changes in limb morphology (e.g., adding flexible wrists) can improve locomotion by reducing interactions of the limbs with previously disturbed material [21], here we find that proper coordination of body-bending and limb placement can also enhance locomotion by enabling the robot to avoid the potentially detrimental effects of disturbed media. These studies provide an example of how robophysics can guide and inform our design of robots that need to move on flowable substrates. This information may be helpful to design an anticipatory control scheme that has memory of a

previously disturbed environment and changes the behavior of the robot according to the predictions of its future state(s).

6.3 Mechanical diffraction and scattering in heterogeneous terrain

In terrestrial locomotion, intermittent contacts and collisions with the environment are typically viewed as detrimental to movement, dissipating energy or even preventing locomotion [25]. However, collisional terradynamics [11] that are properly managed (e.g., appropriate body shape in cockroaches and robots [26]) or properly planned for (e.g., properly timed tail use of a hexapod upon leg collision [27]) can prevent locomotor failure. While mathematical study of hybrid systems has revealed surprises and rich dynamics [4, 28, 29], fewer experimental systems have explored collisional dynamics relevant to locomotion. In fact, collisions can be necessary to generate locomotion and simplify control, from turning an unstable static system into a stable passive dynamic walker [29, 30] to passively stabilizing a rapidly running hexapedal robot across uneven terrain [4]. Repeated collisions with the environment can even lead to novel forms of transport [31].

Snakes and snake-like robots are excellent systems to discover principles of multiterrain control because the long, articulated body provides flexibility and adaptability in locomotion such that limbless animals move proficiently in a wide range of environments [32], including slithering through homogeneous terrain [33], swimming in water [34], gliding in air [35], and navigating through and making use of obstacles and debris in heterogeneous terrain [36, 37]. Although snake-like robots can move in homogeneous environments [10, 38, 39] and are showing improvement in the presence of obstacles [40], they are still limited in their ability to move in clutter, limiting their use in search and rescue [41]. To systematically study how collisions affect limbless locomotion, we took a robophysics approach [5] to build upon previous work [42] to systematically create a statistical understanding of collisions between a limbless locomotor and rigid obstacles it encounters. Our robophysical model snake (shown in Fig. 6.5A), which has 13 segments, is constructed from servo motors connected together with 3D-printed plastic brackets. Joint angles were controlled by prescribing servo motor positions to follow a "serpenoid" curve as a function of segment, i, along the body and as a function of time, t: $\zeta_i(t) = \zeta_{\max} \sin(2\pi i/N - 2\pi f t)$ [39]. For experiments presented here, $\zeta_{\max} = 40$ degrees and $f = 0.15$ Hz. Wheels affixed to the bottom of each segment introduce a frictional anisotropy with the ground and create a strongly preferred direction of motion, enabling the robot to convert the local joint angle displacements into translational motion.

The robot was then placed in a simple heterogeneous terrain: five evenly spaced vertical posts (intended to approximate rocks, twigs, and other immovable obstacles) were rigidly anchored to an otherwise homogeneous substrate; Fig. 6.5A. In each experiment, positions of markers atop each segment were identified and recorded by overhead cameras as a function of time as the robot traveled toward, mechanically interacted with, and subsequently exited, the peg array. This interaction, which

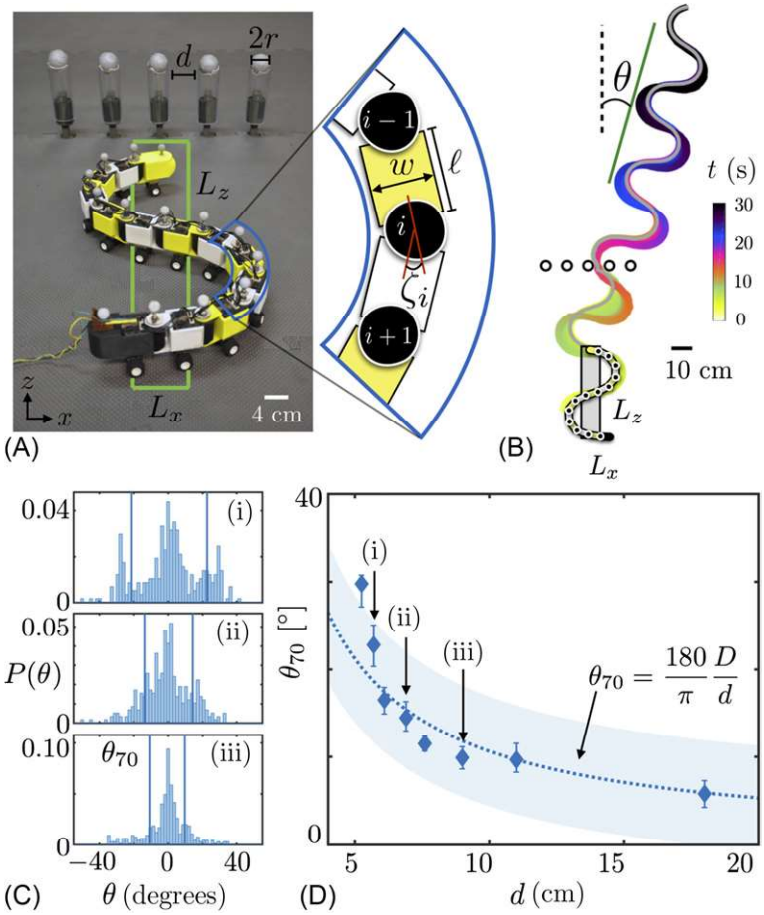

Fig. 6.5 Robotic snake in heterogeneous terrain. (A) A servo-motor-driven robotic snake moves on a flat substrate and interacts with a row of evenly spaced vertical posts (where d is the spacing between the surfaces of adjacent posts). To characterize different robot-post interactions, the initial placement of the robot is varied within the *green box*. A zoomed-in version of three adjacent servo motors (*black circles*) is shown to the *right*. (B) Trajectory of the robot for an experiment with $d = 5.7$ cm. The robot heading is altered by the interaction. *Colored lines* show positions of all segments over time, and the *gray line* shows the trajectory followed by the head. (C) Scattering angle distributions for three postspacings, (i) $d = 5.7$ cm, (ii) $d = 6.9$ cm, (iii) $d = 9.0$ cm, each of which contains at least 300 trials. *Vertical lines* show the angles associated with the outer $\pm 15\%$ of each distribution. (D) θ_{70} vs. d. The *dashed line* shows a fit to the function $\theta_{70} = (180/\pi)(D/d)$ where D is a fit parameter.

depended sensitively on the initial conditions of the robot, rotated the direction of travel and scattered the robot by some angle θ, see Fig. 6.5B. To develop a statistical understanding of all possible collisions and resulting outcomes (for incident heading perpendicular to the array), we varied the initial placement of the robot within a box

(outlined in green in Fig. 6.5A) of lateral and longitudinal dimensions $L_x = d + 2r$ (where d is the postspacing and r is the postradius) and $L_z = v_0 T$, the distance traveled in one undulation cycle.

The interaction with the post array altered the heading of the robot, scattering the trajectory by an angle, θ. We characterize the statistical effects of this "mechanical diffraction" with obstacles on the trajectories of the robot by creating θ-distributions for evenly sampled initial conditions. These distributions are shown for three values of postspacing, d, in Fig. 6.5C. All have a central peak around zero and are symmetric, and as spacing decreases, secondary peaks emerge (particularly when d is small), indicating the presence of preferred reorientations. We quantify how these distributions change with spacing by measuring the quantile angle, θ_{70}, which captures the inner 70% of the distribution (the 70th quantile is akin to a standard deviation, but is more general in that no underlying assumptions about the nature of the distribution are made). These quantile angles are shown as vertical lines on each distribution. As shown in Fig. 6.5D, θ_{70} values decrease with increasing d, confirming that the weight of the distributions shifts inward as spacing increases. Remarkably, this function is captured by a function similar to the Bragg formula used to describe scattering of X-rays, neutrons in crystal lattices.

Our experiments thus reveal that the interaction of a snake-like robot behaves as an active unit with both particle and wave-like properties, a "wavicle" duality [43] observed in subatomic processes (and recently in a hydrodynamic system [44, 45]). In addition to giving us a qualitative picture of how simple undulatory locomotors interact with heterogeneities, these results can provide a statistical understanding of where the robot is likely to travel after interactions with obstacles of a given separation, with smaller d leading to a higher probability of large deflections—that is, a robotic uncertainty principle. This statistical approach provides a starting point for developing simple control schemes which, like our previous work with legged systems [27], can use minimal information from the environment to anticipate and therefore alter the outcome of the interaction.

6.4 Exploring heterogeneous environments with simple strategies

From scattered trees in the forest to rocks in the soil, the natural world is full of homogeneous landscapes punctuated by obstacles that are hard to penetrate. These hybrid dynamics create an inconsistency of interaction that can make model-based robotic control complicated. However, control in such environments needs not be mathematically complex. A biologically relevant example is plant root growth in soil. While much of the soil substrate is homogeneous (e.g., sand or dirt), it can be riddled with rocks and other plant roots as obstacles. As plant roots grow, they must navigate these hybrid dynamics to explore their environment and root themselves deep in the soil. Here, we undertake a robophysical approach inspired by root growth behavior to study how to explore complex environments, and use it as an example of studying simplified control in the face of hybrid dynamics. In search and rescue robotics for example, it is

unclear exactly how much feedback and sensing is required to navigate cluttered environments, for example, a collapsed building [41]. A robophysical approach offers a proof of concept of what can be accomplished when environmental feedback and sensing are virtually nonexistent.

A variety of plant species have roots that exhibit a growing behavior called circumnutation, a circular corkscrew-like motion exhibited by the root tip illustrated in Fig. 6.6A. However, the function of circumnutation is unclear with respect to its natural growth media [46]; does it aid the root in either exploration or substrate penetration? To investigate hypotheses about mechanical penetration benefits of such winding motion, we constructed a simple robotic model of root growth capable of both "growing" and circumnutating into an artificial substrate, in this case, a lattice of rigid obstacles. Existing work observed force reduction effects from circumnutation in homogeneous granular material, for example, soil and sawdust [47]. We specifically sought to test the effects of circumnutation on penetrating heterogeneous substrates, such as rocks and other hard obstacles embedded in soil.

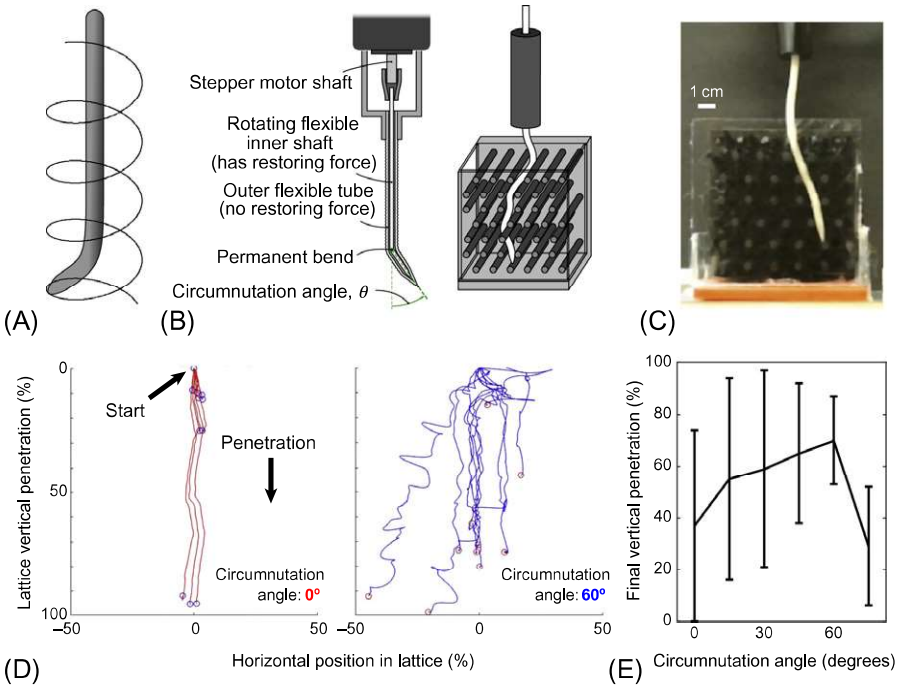

Fig. 6.6 Robophysical investigation into plant root penetration, an example of a simple strategy for exploring heterogeneous environments. (A) Sketch of a plant root tip circumnutating as it grows. (B) Schematic of a robophysical circumnutating root model. (C) Robotic root model navigating an obstacle lattice. (D) Root tip path of multiple lattice penetration trials using two different circumnutation angles (0 degree and 60 degrees). (E) Statistics showing that penetration of the lattice is more consistent and deeper on average with greater circumnutation angle.

The robophysical model, diagrammed in Fig. 6.6B, consists of a rotating flexible root attached to a robotic arm. The flexible root needs compliance to deform around obstacles in its path. The root-like mechanism consists of a rotating inner shaft and a nonrotating outer shaft. The rotating inner shaft is made of 3D-printed nylon, which deflects while having a restorative bending force to restore it to its nominal shape. The nylon was printed to have a bent tip at a predefined angle, which sets the angle of nutation for the root tip. The outer shaft is constructed out of bendable drinking straws to allow deflection without large restorative forces that would return the outer shaft to a nominal shape. While this robophysical model has a number of mechanical differences from root growth (e.g., an intruding shaft instead of a growing tip) it does function as a controlled test for circumnutation as a simplified control scheme.

The inner shaft is mounted to a stepper motor, allowing for simple rotation about the long axis of the root. As a consequence, the tip of the outer shaft draws a circular path without rotating the skin of the outer shaft relative to the world. To facilitate growth, a 6-DOF DENSO robotic arm slowly intrudes the root apparatus down into a chosen substrate. The arm is instrumented with a load cell to measure the forces and torques between the arm and root, which also enables the measurement of energetics for root intrusions. As a heterogeneous substrate for intrusion, we constructed a lattice of acrylic pegs, allowing for the possibility of the root to get "stuck" on the obstacles and halting growth progress. The acrylic obstacles, pictured in Fig. 6.6C, are significantly more rigid than the flexible root and thereby emulate rigid heterogeneities. Progress through the obstacle lattice was monitored using a webcam, which was used to track the root tip over time.

Through multiple statistical trials, we found that increased circumnutation angle allowed for deeper penetration of the obstacle lattice. Fig. 6.6D shows the time-varying path of the mechanism tip both with and without circumnutation, and Fig. 6.6E statistically plots how penetration varies with nutation angle. The mean penetration increased and the variance decreased by forcing the root model to explore via this spiraling motion. Further, the root would rapidly switch contact modes and frictional regimes, making the investigation difficult via use of a computer model. Instead, by examining this phenomenon with a robophysical model, we were able to evaluate the efficacy of simple strategies in spite of these complex interactions. We posit that such techniques can aid robots that must maneuver through complex landscapes that are challenging to map [48] and properly sense [49] and thus plan locomotion. Conversely, this motivates robotic solutions where mechanical compliance can handle the complex dynamics of uncertain heterogeneous environments [50].

6.5 Collective behaviors from mechanical interactions

When many individuals interact, they have the potential to perform tasks collectively that each cannot accomplish alone. We are particularly interested in swarms [51] of functional robots that form emergent behaviors via changes in shape and through collisions. Appropriate coordination of such collisional shape-changing machines could

imitate phases of matter or useful mechanisms on demand. For example, they could lock together to form and break physical chains, or push neighbors away to generate diffusive motion like a gas, or make and break contacts through shape change to generate flowing motion of a collective like a liquid. Thus one could imagine that future robots are actually composed of collectives of robots, such that limbs are periodically stiffening chains and bodies are deforming fluid ensembles. Here we develop simple robots (smart active particles or "smarticles") which have shape-changing capabilities. Through systematic study of properties of ensembles of smarticles, we discover novel emergent properties, including collective drift and diffusion of confined ensembles and ductility of smarticle chains.

Each smarticle is a three-link, two-degree-of-freedom robot (Fig. 6.7C), made from two servos fitted inside a 3D-printed body. Each smarticle is equipped with various sensors, allowing it to sense its environment. These sensors include a current sensing resistor to perceive stress applied to its outer links, photoresistors (located on both front and back) to distinguish various intensities of light, and a microphone which can be used to determine sound levels as well as frequency of sound in the environment. Each smarticle uses an Arduino Pro Mini to control its motors and query the various sensors on its body.

A single smarticle can only control its shape; this means that, depending on the orientation a smarticle is placed in, a single smarticle may not be able to translate or rotate autonomously, which is true when a smarticle is oriented such that its bottom face rests on a surface (pictured in Fig. 6.7A and B). This remains true independent of any positions the arms may move to, or any gait they may perform, where a gait is a periodic trajectory in the smarticle's 2-degree-of-freedom configuration space. One particular gait, called the square gait, is illustrated in Fig. 6.7D. While one smarticle cannot locomote by itself (in this orientation), a collective of smarticles can.

When smarticles are placed together in a group, the collective can be more capable than a solitary smarticle. One particular experiment illustrating this idea is seen in the system we call the "supersmarticle," shown in Fig. 6.7E [52]. A group of five identical smarticles performing identical shape-change sequences are confined along the ground inside an unanchored ring. While each smarticle contained in the unanchored ring cannot individually move, by modulating their shape in such a high-density area, the smarticles interact with their neighbors and the surrounding ring, creating motion of the collective. The mechanical interactions between the smarticles and ring generate Brownian diffusion when tracking the ring's center of geometry. Thus a system composed of nonmotile particles generates motion. The motion generated by these interactions, as described earlier, does not yet have any bias in the movement direction; the final position after a given amount of runtime does not seem to depend strongly on any particular variable.

While the supersmarticle system does indeed move, as a biological analog, we seek to add directional control as well. This shortcoming can be remedied by introducing a single inactive smarticle, depicted in red in Fig. 6.7F, which serves as an asymmetry to the system. The inactive particle will hold a particular shape, specifically a straight rod-like configuration, while the rest of the smarticles continuously change their shape performing a square gait trajectory. This has the effect of creating biased displacement

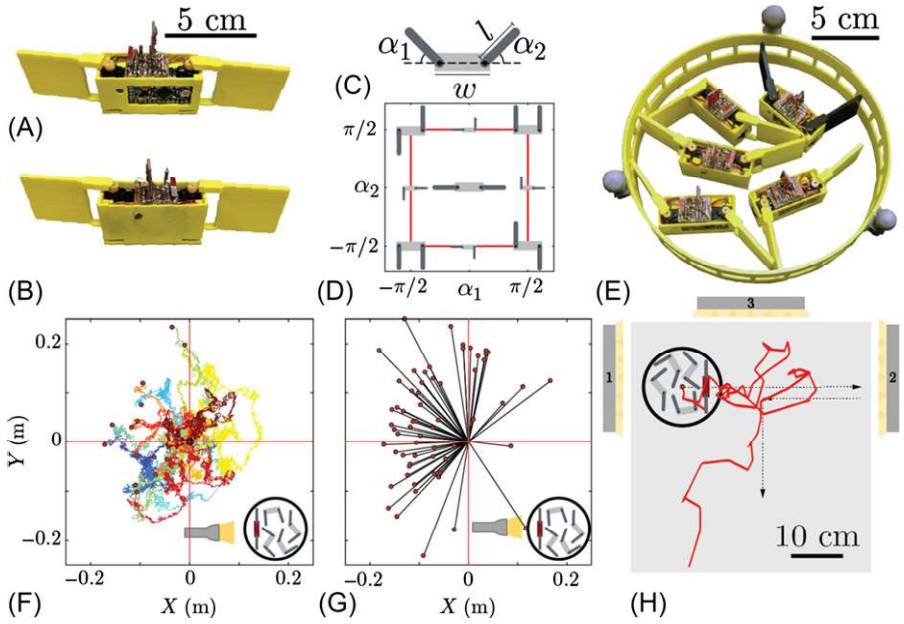

Fig. 6.7 Smarticle system and its collective capabilities. (A) Frontal view of a smarticle robot; (B) smarticle rear view; (C) smarticle schematic with coordinate system and dimension definitions; (D) smarticle square gait with key configurations illustrated; and (E) picture of a light controlled supersmarticle; *gray spheres* are used to track rotation of and translation of ring. (F) Selected experimental trajectories from light controlled photophilic supersmarticle; the control direction is highlighted in the schematic in the lower right, the flashlight directing the supersmarticle to the *left*. (G) Final positions of all light directed photophilic supersmarticle trials. Experimental trials were taken with the flashlight directing the smarticle in different directions and were rotated into a single direction (shown in the *bottom right corner*) to ensure biased motion was not a result of systematic error. (H) Single experimental trajectory shown for a photophobic supersmarticle following a "T" trajectory by sequencing lights as shown in the figure.

of the ring toward the inactive smarticle. We can control which smarticle becomes inactive through the aforementioned light sensors placed on both sides of the smarticle (Fig. 6.7A and B). The control for inactivity is a level threshold; a smarticle is made inactive when a bright enough light is detected. In the supersmarticle, the nearest smarticle to the light source becomes inactive, occluding light from the neighbors behind it; therefore, the asymmetry necessary to generate biased displacement remains in the same location. Results from experiments showing this biased motion in the supersmarticle are depicted in Fig. 6.7F and G. By leveraging this property we are able to create a robot, the supersmarticle, made of other robots, the smarticles, capable of directed displacement in two dimensions, an impossibility for a single smarticle [53].

We next highlight emergent ensemble properties afforded by the smarticles' entanglement ability. In an experiment we call a "smarticle chain," with the setup shown in Fig. 6.8A, we measure the material properties of a group of smarticles. In this experiment we interlink a group of smarticles and with one side of the chain fixed, we apply a constant strain rate ($\dot{\gamma}$) and measure the resulting force. Force-strain tests (Fig. 6.8B), bear features of elastic to plastic behaviors in ductile metal systems [54]: at low strains the smarticle chain exhibits linear elastic properties. As the chain reaches its yield strength, we find physical rearrangement of the smarticles in the chain. After this yield point, the chain displays strain hardening and eventually strain softening behaviors, before finally fracturing. While the smarticle chain's force-strain response looks typical for this particular experiment, this behavior is a result only when the smarticle passively tries to keep its initial "U-shape" position. More exotic force-strain curves can be generated by utilizing the stress-sensing sensors, allowing the smarticles in the chain to actively respond to the applied force.

Despite the smarticle chain exhibiting the stress-strain properties of a normal ductile metal response in the force versus strain, the smarticle chain can display the uncommon property of being "auxetic" [54], where auxetic materials, when strained, expand (rather than shrink) in the transverse direction. Because of its auxetic nature, the properties of the smarticle chain can change in the presence of transverse boundaries. That is, the fracture strength of the chain depends on its confinement. As the

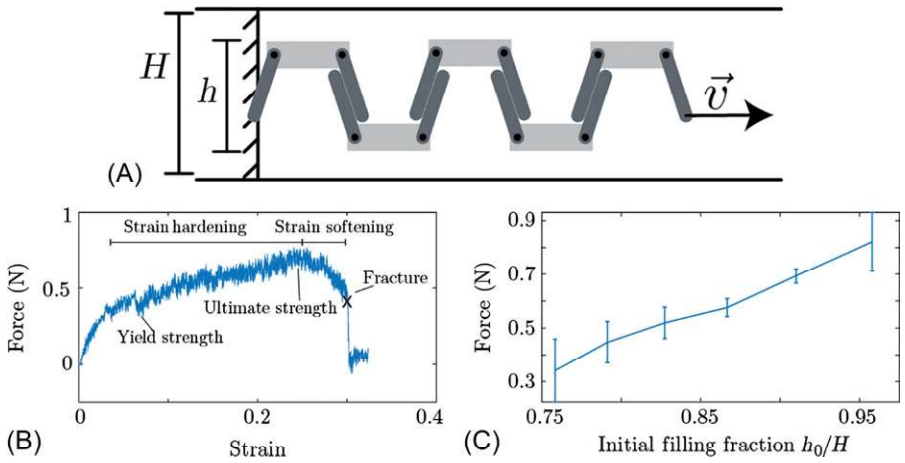

Fig. 6.8 Data from shape-focused smarticle experiments. (A) Schematic of a smarticle chain experiment in the initial configuration; h denotes the instantaneous transverse chain span and H the confining span. (B) Force versus time data measured from the smarticle chain system. The *blue line* represents the force from the chain as it resists strain, where strain is in units of the unstretched chain's length. (C) Force at fracture versus initial linear filling fraction, h_0/H where h_0 is the initial smarticle span. The smarticle chain is auxetic; therefore, the maximum strength measured at fracture will change as a function of H. As initial filling fraction increases, less force is shared between smarticles before a portion of that force is directed to the outer walls rather than being distributed among smarticles alone.

chain is strained, it becomes thicker; depending on the confinement width H shown in Fig. 6.8, it may expand enough to interact with the outer boundary. Upon contact with the boundary the force, which was previously shared between one smarticle and its neighbor, is directed outward into the walls of the system. The lower the strain necessary for the chain's auxetic behavior to cause to fill the system, the more force is offloaded to the wall; therefore, the force the chain can support before fracturing is increased (Fig. 6.8).

Here we demonstrated robotic systems made of other robots, engaging in functions with no centralized intelligence. The supersmarticle collective is more capable than its constituents, able to translate despite being composed of nonmotile individual smarticles. Further, its motion, which is controlled purely through mechanical interactions, can be extrapolated to many already existing systems. Further, we were able to show that shape change in robots allows for interlocking to create materials with specific mechanical properties. We envision that future robots composed of shape changing robots could have features in common with certain biological systems. For example, biomolecular machines perform functions via conformational change in the cooperative "control" of oxygen uptake in hemoglobin molecules [55]; we can imagine that robotic subunits composed of smarticles could function similarly. And most provocatively, inspired by Yim et al. [56], we imagine that the current paradigm for robot construction—robots made of nonrobot components—can change if we adopt a more "metazoan" approach (where organisms are composed of functional living systems, cells). We believe that such modular robots will benefit from appropriate mechanical interactions and shape changes.

6.6 Conclusion

In conclusion, as robots—from life-sized humanoids to nanoswimmers—enter the real world, they will encounter never-studied interactions with their complex environments which, from an engineering perspective, require new mechanics, dynamics, and controls to use/overcome. We have given examples from our work in which treating the robots as experimental tools through systematic study of robots as dynamical systems (rather than as engineered objects to accomplish a particular task) is important to discover and understand novel dynamics. We urge researchers at the interface of robotics and physics to embrace the mindset that one can actually learn from the robots!

In terms of actionable recommendations as to how to train researchers at this interface, we advocate that physicists should interact with roboticists to learn about critical challenges robotics researchers face. Physicists (especially those studying behavior in living systems [57, 58] and active matter [59]) can also benefit from the robotics focus on function, behavior, and goals [60] in dynamical systems, typically not considered in physics. And techniques in machine learning [61, 62] and optimization [63] can point to new physics phenomena. In terms of what physics can bring to robotics, we advocate that roboticists become trained in the practice of experimental science-controlled systematic experiments on simplified systems. While obviously

some robots push the state of the art in materials and design, sufficient down-scoping of goals can lead to better understanding of the system.

We also posit that the integration of physics and robotics can benefit biology. Echoing John Pierce, an engineer who participated in and witnessed the great intersection of solid-state physics and electrical engineering in the mid-20th century:

> *…I will, however, maintain that we can learn at least two things from the history of science. One of these is that many of the most general and powerful discoveries of science have arisen, not through the study of phenomena as they occur in nature, but, rather, through the study of phenomena in man-made devices, in products of technology, if you will. This is because the phenomena in man's machines are simplified and ordered in comparison with those occurring naturally, and it is these simplified phenomena that man understands most easily….*

In proper collaboration, the practitioners of robophysics and integrative biologists could learn from robots to make progress into core principles that govern the astounding capabilities of living systems.

Acknowledgments

The authors would like to thank NSF (PoLS, NRI, CMMI), ARL MAST CTA, ARL RCTA, ARO, DARPA, and the Burroughs Wellcome Fund for supporting aspects of this research. The authors would like to thank J. Aguilar, A. Ames, H. Astley, P. Benfey, B. Bialek, K. Blagoev, M. Buehler, H. Choset, N. Cowan, J. Dai, T. Daniel, K. Diaz, Y. Ding, M. Donelan, R. Dudley, R. Fearing, R. Full, J. Gollub, N. Gravish, Z. Goddard, C. Gong, R. Hatton, N. Hines, H. Jaeger, L. Kadanoff, D. Koditschek, E. Krotkov, G. Lauder, C. Li, V. Linevich, M. MacIver, N. Mazouchova, G. Pratt, A. Rizzi, A. Ruina, G. Sartoretti, S. Sharpe, S. Stanton, H. Swinney, P. Umbanhowar, J. Weitz, K. Wiesenfeld, and A. Zangwill for helpful discussions over the years. The authors also would like to thank all the current and old members in the CRAB Lab, especially P.E. Schiebel, S. Li, M. M-Cooper, E. McCaskey, I. Tomkinson, Z. Stinnett, A. Koh, R. Warkentin, and M. Caveney for assistance with experiments. Some of the thinking on this work was inspired by an NSF/ARO workshop on locomotion in 2012. Certain images in this publication have been obtained by the author(s) from the Wikipedia/Wikimedia website, where they were made available under a Creative Commons license or stated to be in the public domain. Please see individual figure captions in this publication for details. To the extent that the law allows, Elsevier Publishing disclaim any liability that any person may suffer as a result of accessing, using or forwarding the image. Any reuse rights should be checked and permission should be sought if necessary from Wikipedia/Wikimedia and/or the copyright owner (as appropriate) before using or forwarding the image.

References

[1] E. Krotkov, Active perception for legged locomotion: every step is an experiment, in: Proceedings. 5th IEEE International Symposium on Intelligent Control 1990, vol. 1, 1990, pp. 227–232.

[2] R.J. Full, D.E. Koditschek, Templates and anchors: neuromechanical hypotheses of legged locomotion on land, J. Exp. Biol. 202 (23) (1999) 3325–3332.
[3] M.H. Raibert, Legged Robots That Balance, Massachusetts Institute of Technology, Cambridge, MA, 1986.
[4] P. Holmes, R.J. Full, D. Koditschek, J. Guckenheimer, The dynamics of legged locomotion: models, analyses, and challenges, SIAM Rev. 48 (2) (2006) 207–304.
[4a] S. Collins, A. Ruina, R. Tedrake, M. Wisse, Efficient bipedal robots based on passive-dynamic walkers, Science 307 (2005) 1082–1085.
[4b] J. Reher, E.A. Cousineau, A. Hereid, C.M. Hubicki, A.D. Ames, Realizing dynamic and efficient bipedal locomotion on the humanoid robot DURUS, in: IEEE International Conference on Robotics and Automation (ICRA), 2016, pp. 1794–1801.
[5] J. Aguilar, T. Zhang, F. Qian, M. Kingsbury, B. McInroe, N. Mazouchova, C. Li, R. Maladen, C. Gong, M. Travers, R.L. Hatton, H. Choset, P.B. Umbanhowar, D. I. Goldman, A review on locomotion robophysics: the study of movement at the intersection of robotics, soft matter and dynamical systems, Rep. Prog. Phys. 79 (11) (2016) 1–35.
[6] C. Li, P.B. Umbanhowar, H. Komsuoglu, D.E. Koditschek, D.I. Goldman, Sensitive dependence of the motion of a legged robot on granular media, Proc. Natl. Acad. Sci. 106 (9) (2009) 3029–3034.
[7] T. Zhang, F. Qian, C. Li, P. Masarati, A.M. Hoover, P. Birkmeyer, A. Pullin, R.S. Fearing, D.I. Goldman, Ground fluidization promotes rapid running of a lightweight robot, Int. J. Robot. Res. 32 (7) (2013) 859–869.
[8] D.I. Goldman, Colloquium: biophysical principles of undulatory self-propulsion in granular media, Rev. Mod. Phys. 86 (3) (2014) 943–958.
[9] J. Gray, G.J. Hancock, The propulsion of sea-urchin spermatozoa, J. Exp. Biol. 32 (4) (1955) 802–814.
[10] R.D. Maladen, Y. Ding, P.B. Umbanhowar, A. Kamor, D.I. Goldman, Mechanical models of sandfish locomotion reveal principles of high performance subsurface sand-swimming, J. R. Soc. Interface 8 (62) (2011) 1332–1345.
[11] C. Li, T. Zhang, D.I. Goldman, A terradynamics of legged locomotion on granular media, Science 339 (6126) (2013) 1408–1412.
[12] F. Qian, T. Zhang, W. Korff, P.B. Umbanhowar, R.J. Full, D.I. Goldman, Principles of appendage design in robots and animals determining terradynamic performance on flowable ground, Bioinsp. Biomim. 10 (5) (2015) 056014.
[13] H. Askari, K. Kamrin, Intrusion rheology in grains and other flowable materials, Nat. Mater. 15 (12) (2016) 1274.
[14] R.L. Hatton, Y. Ding, H. Choset, D.I. Goldman, Geometric visualization of self-propulsion in a complex medium, Phys. Rev. Lett. 110 (2013) 078101.
[15] F. Qian, T. Zhang, K. Daffon, D.I. Goldman, An automated system for systematic testing of locomotion on heterogeneous granular media, in: International Conference on Climbing and Walking Robots (CLAWAR)2013.
[16] A. Shapere, F. Wilczek, Self-propulsion at low Reynolds number, Phys. Rev. Lett. 58 (1987) 2051–2054, https://doi.org/10.1103/PhysRevLett.58.2051.
[17] J. Dai, H. Faraji, C. Gong, R.L. Hatton, D.I. Goldman, H. Choset, Geometric swimming on a granular surface, in: Robotics: Science and Systems XII, University of Michigan, Ann Arbor, MI, USA, June 18–22, 2016.
[18] C. Gong, D.I. Goldman, H. Choset, Simplifying gait design via shape basis optimization, in: Robotics: Science and Systems XII, University of Michigan, Ann Arbor, MI, USA, June 18–22, 2016.

[19] B. McInroe, H.C. Astley, C. Gong, S.M. Kawano, P.E. Schiebel, J.M. Rieser, H. Choset, R. W. Blob, D.I. Goldman, Tail use improves performance on soft substrates in models of early vertebrate land locomotors, Science 353 (6295) (2016) 154–158.
[20] Y. Ozkan Aydin, B. Chong, C. Gong, J.M. Rieser, J.W. Rankin, K. Michel, A.G. Nicieza, J. Hutchinson, H. Choset, D.I. Goldman, Geometric mechanics applied to tetrapod locomotion on granular media, Lect. Notes Comput. Sci. 10384 (2017) 595–603.
[21] N. Mazouchova, P.B. Umbanhowar, D.I. Goldman, Flipper-driven terrestrial locomotion of a sea turtle-inspired robot, Bioinsp. Biomim. 8 (2) (2013) 026007.
[22] V.A. Harris, On the locomotion of the mud-skipper *Periophthalmus koelreuteri* (Pallas): (Gobiidae), Proc. Zool. Soc. London 134 (1) (1960) 107–135.
[23] C.M. Pace, A.C. Gibb, Mudskipper pectoral fin kinematics in aquatic and terrestrial environments, J. Exp. Biol. 212 (14) (2009) 2279–2286.
[24] B. Chong, Y. Ozkan Aydin, C. Gong, G. Sartoretti, Y. Wu, J.M. Rieser, H. Xing, J. Rankin, K. Michel, A. Nicieza, J. Hutchinson, D.I. Goldman, H. Choset, Coordination of back bending and leg movements for quadrupedal locomotion, Robotics: Science and Systems (RSS), 2018.
[25] J.C. Spagna, D.I. Goldman, P.C. Lin, D.E. Koditschek, R.J. Full, Distributed mechanical feedback in arthropods and robots simplifies control of rapid running on challenging terrain, Bioinsp. Biomim. 2 (1) (2007) 9–18.
[26] C. Li, A.O. Pullin, D.W. Haldane, H.K. Lam, R.S. Fearing, R.J. Full, Terradynamically streamlined shapes in animals and robots enhance traversability through densely cluttered terrain, Bioinsp. Biomim. 10 (4) (2015) 1–24.
[27] F. Qian, D.I. Goldman, Anticipatory control using substrate manipulation enables trajectory control of legged locomotion on heterogeneous granular media, in: T. George, A. K. Dutta, M.S. Islam (Eds.), SPIE Defense and Security, SPIE, 2015.
[28] S.A. Burden, S. Revzen, S.S. Sastry, Model reduction near periodic orbits of hybrid dynamical systems, IEEE Trans. Autom. Control 60 (10) (2015) 2626–2639.
[29] T. McGeer, Passive dynamic walking, Int. J. Robot. Res. 9 (2) (1990) 62–82.
[30] M.J. Coleman, A. Ruina, An uncontrolled walking toy that cannot stand still, Phys. Rev. Lett. 80 (16) (1998) 3658–3661.
[31] T.H. Vose, P. Umbanhowar, K.M. Lynch, Sliding manipulation of rigid bodies on a controlled 6-DoF plate, Int. J. Robot. Res. 31 (7) (2012) 819–838.
[32] B.R. Moon, C. Gans, Kinematics, muscular activity and propulsion in gopher snakes, J. Exp. Biol. 201 (19) (1998) 2669–2684.
[33] P.E. Schiebel, T. Zhang, J. Dai, C. Gong, M. Yu, H.C. Astley, M. Travers, H. Choset, D. I. Goldman, Slithering on sand: kinematics and controls for success on granular media, in: APS Meeting Abstracts, 2016.
[34] G. Taylor, Analysis of the swimming of long and narrow animals, Proc. R. Soc. Lond. Ser A Math. Phys. Sci. 214 (1117) (1952) 158–183.
[35] J.J. Socha, Kinematics: gliding flight in the paradise tree snake, Nature 418 (2002) 603–604.
[36] J. Gray, The mechanism of locomotion in snakes, J. Exp. Biol. 23 (2) (1946) 101–120.
[37] J. Gray, H.W. Lissmann, The kinetics of locomotion of the grass-snake, J. Exp. Biol. 26 (4) (1950) 354–367.
[38] A. Crespi, A.J. Ijspeert, Online optimization of swimming and crawling in an amphibious snake robot, IEEE Trans. Robot. 24 (1) (2008) 75–87.
[39] S. Hirose, A. Morishima, Design and control of a mobile robot with an articulated body, Int. J. Robot. Res. 9 (2) (1990) 99–114.
[40] P. Liljeback, K.Y. Pettersen, Ø. Stavdahl, J.T. Gravdahl, Snake robot locomotion in environments with obstacles, IEEE/ASME Trans. Mechatron. 17 (6) (2012) 1158–1169.

[41] R.R. Murphy, S. Tadokoro, D. Nardi, A. Jacoff, P. Fiorini, H. Choset, A.M. Erkmen, Search and rescue robotics, in: B. Siciliano, O. Khatib (Eds.), Springer Handbook of Robotics, Springer, Berlin, Heidelberg, 2008, pp. 1151–1173.
[42] F. Qian, D.I. Goldman, The dynamics of legged locomotion in heterogeneous terrain: universality in scattering and sensitivity to initial conditions, Robotics: Science and Systems, 2015, pp. 1–9.
[43] V.F. Weisskopf, What is quantum mechanics? Bull. Am. Acad. Arts Sci. 33 (7) (1980) 27–39.
[44] Y. Couder, E. Fort, Single-particle diffraction and interference at a macroscopic scale, Phys. Rev. Lett. 97 (15) (2006) 154101.
[45] J.W.M. Bush, Pilot-wave hydrodynamics, Ann. Rev. Fluid Mech. 47 (2015) 269–292.
[46] S. Mugnai, E. Azzarello, E. Masi, C. Pandolfi, S. Mancuso, Nutation in plants, Rhythms in Plants, Springer, 2015, pp. 19–34.
[47] E.D. Dottore, A. Mondini, A. Sadeghi, V. Mattoli, B. Mazzolai, Circumnutations as a penetration strategy in a plant-root-inspired robot, in: 2016 IEEE International Conference on Robotics and Automation (ICRA), 2016, pp. 4722–4728.
[48] H. Durrant-Whyte, T. Bailey, Simultaneous localization and mapping: part I, IEEE Robot. Autom. Mag. 13 (2) (2006) 99–110.
[49] M. Hoy, A.S. Matveev, A.V. Savkin, Algorithms for collision-free navigation of mobile robots in complex cluttered environments: a survey, Robotica 33 (3) (2015) 463–497.
[50] U. Saranli, M. Buehler, D.E. Koditschek, Rhex: a simple and highly mobile hexapod robot, Int. J. Robot. Res. 20 (7) (2001) 616–631.
[51] M. Brambilla, E. Ferrante, M. Birattari, M. Dorigo, Swarm robotics: a review from the swarm engineering perspective, Swarm Intell. 7 (1) (2013) 1–41.
[52] S. Cannon, J.J. Daymude, W. Savoie, R. Warkentin, S. Li, D.I. Goldman, D. Randall, A. W. Richa, Phototactic supersmarticles, CoRR (2017). http://arxiv.org/abs/1711.01327.
[53] R. Warkentin, W. Savoie, D.I. Goldman, Locomoting robots composed of immobile robots. IRC Proc. (2018), https://doi.org/10.3182/20080706-5-KR-1001.01833.
[54] W.D. Callister, D.G. Rethwisch, Materials Science and Engineering: An Introduction, ninth ed., Wiley, Hoboken, NJ, 2014.
[55] W.A. Eaton, E.R. Henry, J. Hofrichter, A. Mozzarelli, Is cooperative oxygen binding by hemoglobin really understood? Nat. Struct. Mol. Biol. 6 (4) (1999) 351.
[56] M. Yim, W.M. Shen, B. Salemi, D. Rus, M. Moll, H. Lipson, E. Klavins, G.S. Chirikjian, Modular self-reconfigurable robot systems [grand challenges of robotics], IEEE Robot. Autom. Mag. 14 (1) (2007) 43–52.
[57] G.J. Berman, Measuring behavior across scales, BMC Biol. 16 (1) (2018) 23.
[58] A.E.X. Brown, B. de Bivort, Ethology as a physical science, Nat. Phys. (2018) 1.
[59] M.C. Marchetti, J.F. Joanny, S. Ramaswamy, T.B. Liverpool, J. Prost, M. Rao, R. A. Simha, Hydrodynamics of soft active matter, Rev. Mod. Phys. 85 (3) (2013) 1143.
[60] E. Roth, S. Sponberg, N.J. Cowan, A comparative approach to closed-loop computation, Curr. Opin. Neurobiol. 25 (2014) 54–62.
[61] P. Baldi, P. Sadowski, D. Whiteson, Searching for exotic particles in high-energy physics with deep learning, Nat. Commun. 5 (2014) 4308.
[62] C.E. Rasmussen, Gaussian processes in machine learning, Advanced Lectures on Machine Learning, Springer, 2004, pp. 63–71.
[63] C.M. Hubicki, J.J. Aguilar, D.I. Goldman, A.D. Ames, Tractable terrain-aware motion planning on granular media: an impulsive jumping study, in: 2016 IEEE/RSJ International Conference on Intelligent Robots and Systems (IROS), IEEE, 2016, pp. 3887–3892.